

---

# Benford's law: what does it say on adversarial images?\*

João G. Zago<sup>1</sup> · Fabio L. Baldissera<sup>1</sup> ·  
Eric A. Antonelo<sup>1</sup> · Rodrigo T. Saad<sup>1</sup>

**Abstract** Convolutional neural networks (CNNs) are fragile to small perturbations in the input images. These networks are thus prone to malicious attacks that perturb the inputs to force a misclassification. Such slightly manipulated images aimed at deceiving the classifier are known as adversarial images. In this work, we investigate statistical differences between natural images and adversarial ones. More precisely, we show that employing a proper image transformation and for a class of adversarial attacks, the distribution of the leading digit of the pixels in adversarial images deviates from Benford's law. The stronger the attack, the more distant the resulting distribution is from Benford's law. Our analysis provides a detailed investigation of this new approach that can serve as a basis for alternative adversarial example detection methods that do not need to modify the original CNN classifier neither work on the raw high-dimensional pixels as features to defend against attacks.

**Keywords** Benford's law · adversarial attacks · convolutional neural networks · adversarial detection

## 1 Introduction

Convolutional neural networks (CNN) are highly successful in image classification tasks [21]. However, they are not robust to small perturbations in the input [3,

---

\* This paper is a draft submitted to a journal and currently being reviewed.

João G. Zago  
E-mail: joao.zago@posgrad.ufsc.br

Fabio L. Baldissera  
E-mail: fabio.baldissera@ufsc.br

Eric A. Antonelo  
E-mail: eric.antonelo@ufsc.br

Rodrigo T. Saad  
E-mail: rsaad@das.ufsc.br

<sup>1</sup> Department of Automation and Systems, UFSC. Florianópolis, Santa Catarina. Brazil

22, 25], i.e., slight changes in the values of the pixels of an input image might result in completely different classification outputs. Malicious attacks can explore this fragility of neural networks, giving rise to the so-called adversarial images [3]. This difficulty to identify manipulated images raises concerns for the application of neural networks in domains where safety is of primary interest [5, 7].

There are several different approaches proposed in the literature to address this problem. They can be grouped into two major categories: a) network-centered, whose aim is to decrease the neural network vulnerability to adversarial images [3, 10, 13, 16, 22, 24]; b) input-centered, where the goal is to detect adversarial images [4, 7, 12, 14, 20].

This paper is related to approach (b) mentioned above, because we propose the use of Benford’s Law (BL), also known as the First Digit Law (FDL), to expose adversarial images. After all, the findings we present here could be used to detect adversarial images. BL states the behavior of the first digit distribution from a natural data set. According to this law, the leading digit distribution of real-world data can be captured by a logarithmic function, described later in detail. The idea of applying BL in the context of adversarial image recognition was inspired by the successful use of BL in other domains, such as in image forensics, to detect frauds [1, 23] and image compression [15, 18], for instance.

In this work, we show that adversarial images devised by state-of-the-art attack algorithms display a leading digit distribution of the pixel values that deviate from that of natural images. While natural images seem to adhere to the FDL, the same is not valid for their corresponding perturbed images.

To the best of our knowledge, this is the first time BL is used for this purpose. Our main contribution in this paper is to provide a solid empirical analysis that leads to the following claims: a) adversarial images, different from natural ones, tend to deviate significantly from BL; b) this deviation is greater for attack algorithms based on infinite-norm perturbations; c) deviations from Benford’s Law increase with the magnitude of the designed perturbation; d) in some cases, adversarial attacks can be anticipated even before the perturbed image becomes adversarial, that is, a deviation from BL takes place during the formation of an attack; and, e) Another fundamental characteristic of this new approach is that it produces a computationally cheap low-dimensional input feature that could be used for adversarial image detection.

We organized this work as follows. Section 2 presents the method to compute the deviation of adversarial and natural images with respect to the distribution given by BL. In Section 3, we describe the experimental setup used to generate the data that supports our claims. Major results are presented in Section 4, while conclusions and future perspectives are given in Section 5.

## 2 Methods

In this paper, we may refer to an input image  $x$  both as a vector ( $x \in \mathbb{R}^n$ ) or as a 2-D matrix ( $x \in \mathbb{R}^{n \times m}$ ), to simplify notation. Given any image  $x$ , we summarize our approach as follows: a) compute the gradient of  $x$ , here denoted  $T(x)$ ; then b) get the frequency of the first digits of  $T(x)$ ; c) compare, through the Kolmogorov-Smirnov test, the distribution got in (b) with the one given by Benford’s law. The

procedure encompassed by steps (a)-(c) is shown in Figure 1. We now detail each of these steps in the sections that follow.

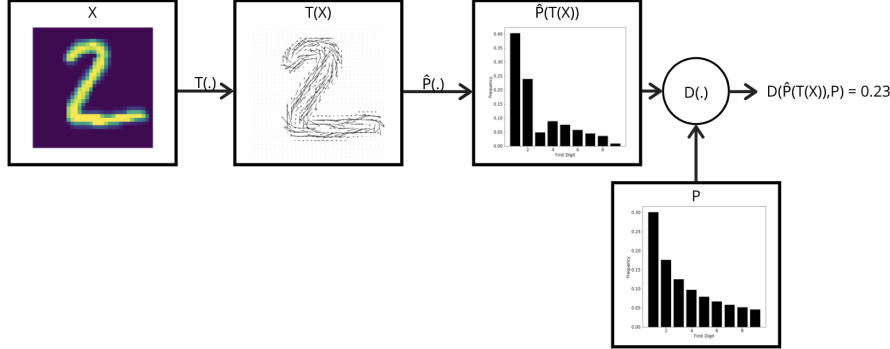


Fig. 1: Overview of the proposed approach, composed of three steps: a) transformation of the image  $x$ , represented by the mapping  $T(\cdot)$ ; b) a statistical analysis of  $T(x)$ , denoted by  $\hat{P}$  and c) a comparison of  $\hat{P}$  with a distribution of reference  $P$ .

## 2.1 Benford's Law

Benford's Law or the First Digit Law states that, across different domains, the distribution of the leading digits of numerical data follows a similar pattern, namely, the one given by Equation 1:

$$P(d) = \log_{10} \left( 1 + \frac{1}{d} \right) \quad (1)$$

Figure 2 portrays the First Digit distribution, as proposed in BL. Pixel-based images rarely follow BL [6]. However, for certain transformations, the transformed images do. Two examples of such transformations are: the gradient magnitude of the input image [6] and the Discrete Cosine Transformation (DCT) [17]. We employed the former, presented next, to map images such that the natural ones behave as in BL.

## 2.2 Image Transformation: Gradient Magnitude

Given an input image  $x \in \mathbb{R}^{n \times m}$ , we compute its gradient  $G(x)$  according to Equation 2 below:

$$G(x)_{i,j} = \sqrt{G_{e_1}(x)_{i,j}^2 + G_{e_2}(x)_{i,j}^2}, \quad (2)$$

where  $G(x)$  is the gradient magnitude;  $i$  and  $j$  are indices indicating each pixel value;  $G_{e_1}(x)$  and  $G_{e_2}(x)$  are the horizontal and vertical components of the gradient approximation, given by:

$$G_{e_1}(x) = x * K_{e_1}, \quad G_{e_2}(x) = x * K_{e_2} \quad (3)$$

which are computed using the following Sobel filters  $K_{e_1}$  and  $K_{e_2}$  for the convolution operation with the input image:

$$K_{e_1} = \begin{bmatrix} -1 & 0 & 1 \\ -2 & 0 & 2 \\ -1 & 0 & 1 \end{bmatrix}, K_{e_2} = \begin{bmatrix} -1 & -2 & -1 \\ 0 & 0 & 0 \\ 1 & 2 & 1 \end{bmatrix}$$

The discrete convolution operation, employed in Equation 3 for the approximation of the gradient in both directions, is given by:

$$(x * K)_{i,j} = \sum_{o=1}^O \sum_{p=1}^P x_{i-o,j-p} K_{o,p} \quad (4)$$

where  $K$  represents, generically, both of the Sobel filters;  $O$  and  $P$  are the number of rows and columns, respectively, relative to  $K$ .

### 2.3 Computing the First Digit Distribution

Given the transformed image  $T(x)$ , we aim to calculate its associated first digit distribution. Firstly, we get the leading digit of each of its pixel values. The first digits of  $T(x)$  are denoted as  $F(T(x))$  (e.g.,  $F$  will output 1 given the pixel value 176, and 5 given 54). Then the frequency for each digit  $d \in \{1, \dots, 9\}$  is computed, forming a distribution  $\hat{P}(d)$ , satisfying  $\sum_{d=1}^9 \hat{P}(d) = 1$ . Note that  $T(x)$  correspond to  $G(x)$  in this work.

### 2.4 Comparing two distributions: the Kolmogorov-Smirnov test

Given two distributions, one may use the Kolmogorov-Smirnov test to compute how much these distributions diverge. This test evaluates the distance between two empirical distributions, or between the theoretical and an empirical distribution.

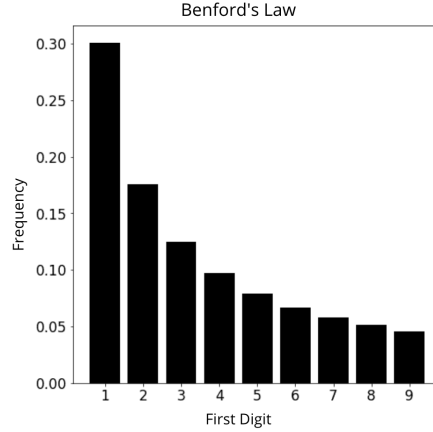


Fig. 2: First digit distribution as in Benford's Law

To assess the difference between the empirical distribution  $\hat{P}$  and the theoretical distribution  $P$ , given by BL, we employed this test, by calculating the KS statistic between these distributions, denoted as  $D^{KS}(\hat{P}, P)$ , using the formula below:

$$D^{KS}(p, q) = \sup |Acc(p) - Acc(q)|, \quad (5)$$

where  $Acc$  returns the accumulated distribution of its given input distribution; and  $p$  and  $q$  correspond to the distributions.

### 3 Experimental Setup

In this section, we present the setup employed to analyse the deviation of adversarial images from the Benford’s distribution. We briefly present the selected image data sets as well as the employed CNN architecture and training parameters (when applied). The adversarial attacks used in our experiments are also listed.

#### 3.1 Data sets

Three different image data sets are considered in this work:

- MNIST: data set containing grayscale images for digits from 0 to 9 [11];
- CIFAR10: data set composed of 10 different classes of RGB images [9];
- ImageNet: data set composed of 1000 different classes of RGB images [2].

#### 3.2 CNNs under attack

We employed a different CNN model architecture for each of the data sets. The CNNs employed to classify images from the MNIST (Table 1) and CIFAR10 (VGG16 [19]) data sets were trained from scratch, while a benchmark network was employed for the data from ImageNet (VGG19 [19]).

For the MNIST data set, the ADAM [8] optimization algorithm was employed in the training procedure with a learning rate of  $1e-3$ ,  $\beta_1 = 0.9$ ,  $\beta_2 = 0.999$  and  $\epsilon = 1e-08$ . The classifier was trained for about 50 epochs, reaching a training accuracy of about 99.29% and for the test set 97.03%.

For training the CIFAR10 classifier, the optimization algorithm employed in the training procedure was the Gradient Descent with momentum, with a learning rate of  $1e-3$  and a momentum of 0.9. The training procedure took about 50 epochs, reaching a training accuracy of about 99.74% and for the test set 80.11%.

#### 3.3 Adversarial Attacks

We employed two different adversarial attack algorithms, the FGSM [3] and the PGD [13], to generate the adversarial examples associated with each of the CNN classifiers presented in the previous section. Both attacks are classified as white-box.

Table 1: Neural Network Architecture - MNIST

Layer	Type	Dimensions
0	Input	(32x32x3)
1	Conv(3x3)-64	(32x32x64)
2	Conv(3x3)-64	(32x32x64)
3	Batch Normalization	(32x32x64)
4	Max Pooling(2x2)	(16x16x64)
5	Conv(3x3)-128	(16x16x128)
6	Conv(3x3)-128	(16x16x128)
7	Batch Normalization	(16x16x128)
8	Max Pooling(2x2)	(8x8x128)
9	Conv(3x3)-256	(8x8x256)
10	Conv(3x3)-256	(8x8x256)
11	Batch Normalization	(8x8x256)
12	Max Pooling(2x2)	(4x4x256)
13	Fully Connected	(2048)
14	Batch Normalization	(2048)
15	Fully Connected	(2048)
16	Fully Connected	(10)

The Fast Gradient Sign Method attack [3] was designed to generate adversarial examples in a one-step iterative process. This attack method uses internal information from the classifier and has access to the training set to generate perturbed images. The perturbation is computed by applying the gradient of the loss function  $J(\theta, x, y)$  usually employed for training a neural net classifier, where  $x$  is a given input image and  $y$  the target output;  $\theta$  represents the weights of a neural net. But, here, the gradient of the loss function is taken with respect to the input image. Then, the adversarial perturbation for each sample  $x$  is computed by Equation (6):

$$x^* = x + \epsilon \operatorname{sign}(\nabla_x J(\theta, x, y)) \quad (6)$$

where  $\epsilon$  is the magnitude of the perturbation and  $x^*$  is the new image which was perturbed using only the sign of the gradient in a direction to maximize the loss function. Note that the same loss function was minimized by taking the gradient with respect to the neural network parameters during its training phase.

### 3.4 Experiments Description

To analyze the deviation between the first digit distributions of the original and the adversarial images, we employed the following steps:

1. Select 1000 random images from the test set for each of the tested data sets (MNIST, CIFAR10, and ImageNet);
2. Attack each of these selected images with the employed adversarial attack algorithms (FGSM and PGD);
3. Compute transformation of the inputs by evaluating the gradient magnitude of the original and the corresponding generated adversarial examples, according to Equation 2;
4. Compute the first digit distribution,  $\hat{P}$ , for the transformed input;

5. Evaluate the KS statistic for the first digit distribution of each original and adversarial example, compared to the original first digit distribution proposed by BL (Equation 5);
6. Evaluate the Kullback-Leibler (KL) divergence between the first digit distribution of each original and adversarial example, compared to the theoretical distribution (Equation 7), to compare with the Kolmogorov-Smirnov test.

$$D^{KL}(p, q) = \sum_{d=1}^9 p(d) \log(p(d) \div q(d)) \quad (7)$$

## 4 Results

### 4.1 Adversarial images tend to significantly deviate from Benford's Law

The comparison between the KS test for the adversarial examples and the original examples generated by the PGD using both the  $\|\cdot\|_\infty - norm$  and  $\|\cdot\|_2 - norm$  approaches, presented in Figure 3, indicates that most of the generated adversarial examples had a higher KS statistic value compared to the theoretical FDL.

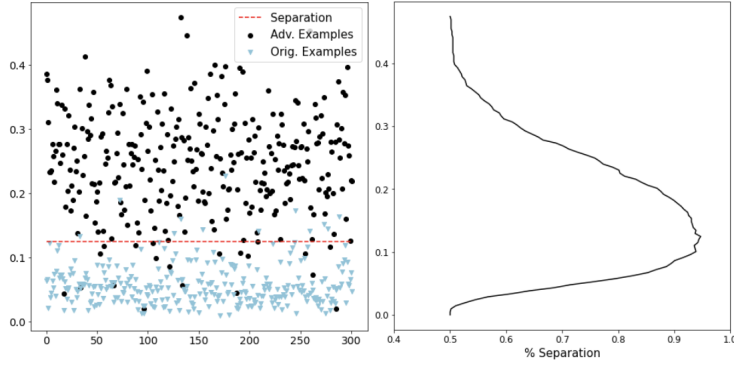
We also have the relation of the separation percentage and the KS statistic for both cases, where it was possible to reach 94.7% for the adversarial examples generated by the  $\|\cdot\|_\infty - norm$  PGD attack, and 81.8% for the adversarial examples generated by the  $\|\cdot\|_2 - norm$  PGD attack. These results corroborate the fact that the first digit distribution of a transformed input image deviates from the adversarial images associated with it.

### 4.2 Images generated by $\|\cdot\|_\infty - norm$ attacks deviate more from the Benford's distribution than those devised by $\|\cdot\|_2 - norm$ attacks

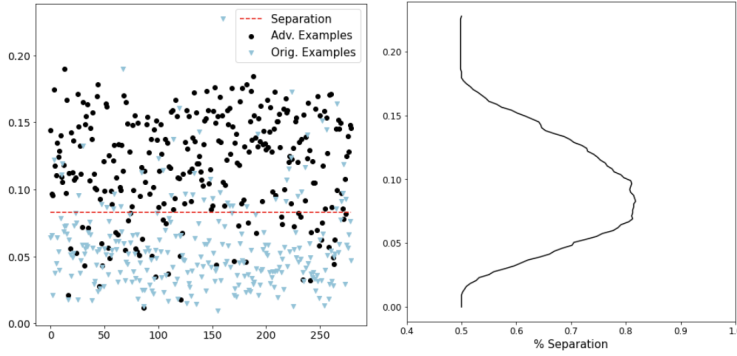
Figure 3 presents a comparison between the deviation calculated for adversarial examples generated by an  $\|\cdot\|_\infty - norm$  and a  $\|\cdot\|_2 - norm$  attacker. By analyzing the separation percentage for different values of the KS test, it is possible to visualize that the deviation of the  $\|\cdot\|_\infty - norm$  attacker is greater, which results in a higher reachable separation percentage. These results remained invariant for different image data sets.

### 4.3 The deviation from Benford's distribution increases with the magnitude of the attack's perturbation

We have that the proposed approach makes it possible to separate adversarial examples from clean examples, for different values of  $\epsilon$ , as presented in Figure 4. Moreover, by comparing the divergence for higher values of  $\epsilon$ , we notice that the higher the perturbation imposed to the original example, the more explicitly separated these sets become. This behavior is invariant for all the data sets employed during the experiments.



(a) Represents the adversarial examples generated using the  $\|\cdot\|_\infty - norm$  PGD attack



(b) Results associated with the examples crafted with the  $\|\cdot\|_2 - norm$  PGD attack

Fig. 3: Scatter plot of the KS statistic for adversarial and clean examples. The first column comprises the dispersion of the KS statistic for both adversarial and original examples. The second column contains the behavior of the separation percentage concerning the KS test value.

Despite the non-intuitive relation between the increment on the magnitude of the imposed perturbation and the distribution of the first digit, the higher the perturbation designed, or artificiality imposed by the  $\|\cdot\|_\infty - norm$  attack, the easier it is to identify adversarial examples by comparing the first digit distribution with the distribution proposed by Benford’s Law, as proposed in this paper.

#### 4.4 The increment on the deviation can be identified during the attack

We have that the KS statistic overcame the separation limit computed according to the Figure 3 before turning into an adversarial example, for some of the examples presented in Figure 5. This limit consists of the separation value with a higher success rate for adversarial and clean examples.

This result shows that, by analyzing the KS test value, it may be possible to identify that a neural network is under attack, i.e., that an attacker is using output



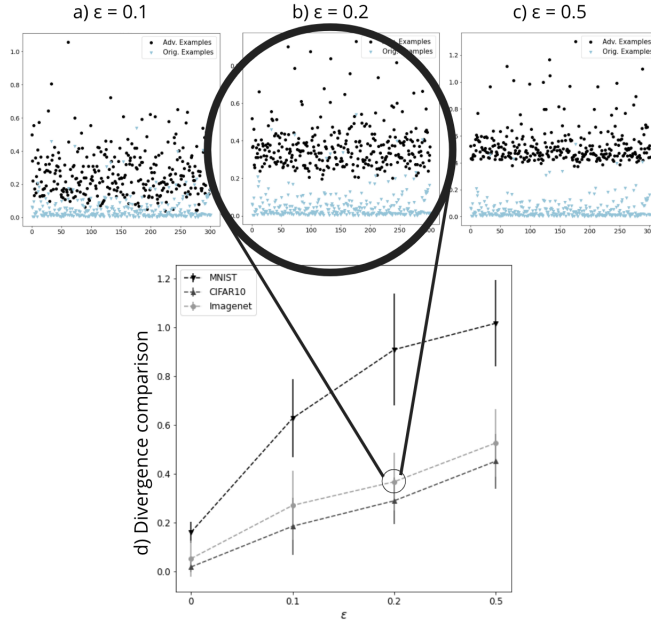


Fig. 4: Images a), b), and c) present the Kullback-Leibler divergence between the first digit distribution of the gradient magnitude for the adversarial and the original examples, concerning the original distribution proposed by Benford's Law, where the attacked images were sampled from the Imagenet data set. The adversarial examples were designed by the  $\|\cdot\|_\infty$ -norm FGSM attack with  $\epsilon$  equal to 0.1, 0.2 and 0.5, respectively. Image d) contains the mean and standard deviation for the KL-divergence while varying the  $\epsilon$  for three different data sets.

information to design a perturbation that will change the classification associated with the original input image.

#### 4.5 The Kolmogorov-Smirnov test performed in comparison to the Kullback-Leibler divergence

We employed the PGD attack, under  $\|\cdot\|_2$ -norm and  $\|\cdot\|_\infty$ -norm, for comparing the maximum separation percentage while using KS test and the KL divergence as it is considered the strongest first-order attack [13]. The results, presented in Table 2, indicate that there is a significant increment in the separation percentage when applying the KS test under both of the PGD approaches.

This analysis suggests that the KS test is more sensitive to the deviations on the first digit distribution because it reaches a higher separation percentage using the same amount of information given for the KL-divergence.

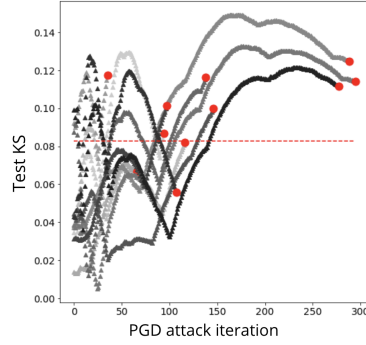


Fig. 5: Behavior of the KS test along the attack iteration of the 2 – *norm* implementation of the PGD attack for 11 examples from the Imagenet data set.

Table 2: Maximum separation percentage comparison between the Kullback-Leibler divergence and the Kolmogorov-Smirnov statistics.

	KL-divergence	KS test
PGD $\infty$ – <i>norm</i>	90.23%	94.70%
PGD 2 – <i>norm</i>	66.96%	81.79%

## 5 Conclusion

In this paper, we proposed a new approach by which we can detect adversarial images without changing parameters or the functioning of the classifier, nor training a new classifier to detect adversarial images. Instead, our approach relies on computing the first digit distribution of the pixel values for classifier input images. The assumption is that adversarial images do not follow Benford’s law (BL) as natural images do.

Our approach comprises applying the Kolmogorov-Smirnov statistic between the first digit distribution of CNN’s input image and the fixed distribution from BL (after applying a suitable transformation to the given image). Specifically, we have shown that the leading digit distribution of adversarial images generated by FGSM and PGD attack methods differs significantly from the corresponding distribution observed in unaltered images: the former deviates significantly more from BL when compared to the latter. This deviation tends to become higher as the magnitude of the perturbation increases (for the FGSM attack).

Besides, one can use our approach to anticipate a potential undergoing attack since we have observed that, in many cases, the deviation given by the KS statistic reaches the separation threshold before the image becomes adversarial.

Future works include devising a sophisticated adversarial image detector, based on the output of the KS statistic test, which can be used as a low-dimensional input feature instead of the whole high-dimensional image. For instance, it is possible to divide an image such that multiple KS statistics tests are obtained from the same input image, providing a more refined, informative view of the deviation caused by the attack perturbation.

Preliminary tests on the repeated application of the gradient transformation for a given image (e.g., two times) improved the results while employing the KL divergence instead of the KS test. This should be investigated in upcoming research. Different adversarial attack methods should be considered, mainly black-box algorithms or those that perturb only a few pixels.

**Acknowledgements** This work has been partially supported by CAPES - The Brazilian Agency for Higher Education (Finance Code 001), project PrInt CAPES-UFSC "Automation 4.0".

## References

1. Deckert, J., Myagkov, M., Ordeshook, P.C.: Benford's law and the detection of election fraud. *Political Analysis* **19**(3), 245–268 (2011)
2. Deng, J., Dong, W., Socher, R., Li, L.J., Li, K., Fei-Fei, L.: ImageNet: A Large-Scale Hierarchical Image Database. In: *CVPR09* (2009)
3. Goodfellow, I.J., Shlens, J., Szegedy, C.: Explaining and harnessing adversarial examples. *CoRR abs/1412.6572* (2015)
4. Grosse, K., Manoharan, P., Papernot, N., Backes, M., McDaniel, P.: On the (statistical) detection of adversarial examples. *CoRR abs/1702.06280* (2017)
5. Huang, X., Kwiatkowska, M., Wang, S., Wu, M.: Safety verification of deep neural networks. In: *International Conference on Computer Aided Verification*, pp. 3–29. Springer (2017)
6. Jolion, J.M.: Images and benford's law. *Journal of Mathematical Imaging and Vision* **14**(1), 73–81 (2001)
7. Katz, G., Barrett, C., Dill, D.L., Julian, K., Kochenderfer, M.J.: Reluplex: An efficient smt solver for verifying deep neural networks. In: *International Conference on Computer Aided Verification*, pp. 97–117. Springer (2017)
8. Kingma, D., Ba, J.: Adam: A method for stochastic optimization. *International Conference on Learning Representations* (2014)
9. Krizhevsky, A., Hinton, G.: Learning multiple layers of features from tiny images. University of Toronto (2012)
10. Kurakin, A., Goodfellow, I., Bengio, S.: Adversarial machine learning at scale. In: *International Conference on Learning Representations, ICLR 2016* (2016)
11. LeCun, Y., Cortes, C.: MNIST handwritten digit database (2010). URL <http://yann.lecun.com/exdb/mnist/>
12. Lu, J., Issaranon, T., Forsyth, D.: Safetynet: Detecting and rejecting adversarial examples robustly. In: *Proceedings of the IEEE International Conference on Computer Vision*, pp. 446–454 (2017)
13. Madry, A., Makelov, A., Schmidt, L., Tsipras, D., Vladu, A.: Towards deep learning models resistant to adversarial attacks. In: *International Conference on Learning Representations, ICLR 2018* (2018)
14. Metzen, J.H., Genewein, T., Fischer, V., Bischoff, B.: On detecting adversarial perturbations. In: *Proceedings of 5th International Conference on Learning Representations (ICLR)* (2017)
15. Milani, S., Fontana, M., Bestagini, P., Tubaro, S.: Phylogenetic analysis of near-duplicate images using processing age metrics. In: *2016 IEEE International Conference on Acoustics, Speech and Signal Processing (ICASSP)*, pp. 2054–2058. IEEE (2016)
16. Papernot, N., McDaniel, P., Wu, X., Jha, S., Swami, A.: Distillation as a defense to adversarial perturbations against deep neural networks. In: *2016 IEEE Symposium on Security and Privacy (SP)*, pp. 582–597. IEEE (2016)
17. Pérez-González, F., Heileman, G.L., Abdallah, C.T.: Benford's law in image processing. In: *2007 IEEE International Conference on Image Processing*, vol. 1, pp. I–405. IEEE (2007)
18. Pevny, T., Fridrich, J.: Detection of double-compression in jpeg images for applications in steganography. *IEEE Transactions on information forensics and security* **3**(2), 247–258 (2008)

19. Simonyan, K., Zisserman, A.: Very deep convolutional networks for large-scale image recognition. In: 3rd International Conference on Learning Representations, ICLR 2015, San Diego, CA, USA, May 7-9, 2015, Conference Track Proceedings (2015)
20. Song, Y., Kim, T., Nowozin, S., Ermon, S., Kushman, N.: Pixeldefend: Leveraging generative models to understand and defend against adversarial examples. CoRR **abs/1710.10766** (2017)
21. Szegedy, C., Ioffe, S., Vanhoucke, V., Alemi, A.A.: Inception-v4, inception-resnet and the impact of residual connections on learning. In: Proceedings of the Thirty-First AAAI Conference on Artificial Intelligence, AAAI’17, p. 4278–4284. AAAI Press (2017)
22. Szegedy, C., Zaremba, W., Sutskever, I., Bruna, J., Erhan, D., Goodfellow, I.J., Fergus, R.: Intriguing properties of neural networks. CoRR **abs/1312.6199** (2014)
23. Tödter, K.H.: Benford’s law as an indicator of fraud in economics. German Economic Review **10**(3), 339–351 (2009)
24. Tramèr, F., Kurakin, A., Papernot, N., Goodfellow, I., Boneh, D., McDaniel, P.: Ensemble adversarial training: Attacks and defenses. In: International Conference on Learning Representations, ICLR 2017 (2017)
25. Wang, Z.M., Gu, M.T., Hou, J.H.: Sample based fast adversarial attack method. Neural Processing Letters **50**(3), 2731–2744 (2019)